European Journal of Pharmaceutics and Biopharmaceutics 74 (2010) 2–13

Contents lists available at ScienceDirect

European Journal of Pharmaceutics and Biopharmaceutics

journal homepage: www.elsevier.com/locate/ejpb

Review article

# Utilising atomic force microscopy for the characterisation of nanoscale drug delivery systems

Johannes Sitterberg [a], Aybike Özcetin [a], Carsten Ehrhardt [b], Udo Bakowsky [a,*]

[a] Department of Pharmaceutical Technology and Biopharmacy, Philipps Universität Marburg, Marburg, Germany
[b] School of Pharmacy and Pharmaceutical Sciences, Trinity College Dublin, Dublin, Ireland

ARTICLE INFO

*Article history:*
Received 12 February 2009
Accepted in revised form 9 September 2009
Available online 13 September 2009

*Keywords:*
AFM
SFM
Liposomes
Nanoparticles
Gene vehicle
Drug delivery systems

ABSTRACT

The introduction of atomic force microscopy (AFM) techniques has revolutionised our ability to characterise colloidal objects. AFM allows the visualisation of samples with sub-nanometre resolution in three dimensions in atmospheric or submerged conditions. Nanomedical research is increasingly focused on the design, characterisation and delivery of nano-sized drug carriers such as nanoparticles, liposomes and polyplexes, and this review aims to highlight the scope and advantages of AFM in this area.

A significant amount of work has been carried out in drug delivery system (DDS) research in recent years using a large variety of techniques. The use of AFM has enabled us to directly observe very small objects without the need of a cumbersome and potentially contaminating sample preparation. Thus, nanoscale DDS can be investigated in a controlled environment without the necessity of staining or drying. Moreover, intermittent contact mode AFM allows the investigation of soft samples with minimal sample alteration; phase imaging allows accessing information beyond the sample's topography and also differentiating between different materials, and force spectroscopy experiments help us to understand the intrinsic structure of DDS by recording the elastic or adhesion behaviour of particles. Hence, AFM enables us accessing information which is hardly available by other experimental techniques. It has provided invaluable information about physicochemical properties and helped to shed light on the area of nanoscale drug delivery and will, with more and more sophisticated equipment becoming available, continue to add to our understanding of the behaviour of nanoscale DDS in the future.



## 1. Introduction

The development of biopharmaceuticals with short biological half-lives (e.g., peptides, proteins and nucleic acids) and novel highly active drugs with potentially severe side effects (e.g., immunosuppressants, glucocorticosteroids and chemotherapeutics) has led to an increased interest in methods delivering and restricting these compounds to the desired site of action. In addition, these compounds often suffer from poor biopharmaceutical properties (e.g., solubility, stability and biodistribution) that are necessary to make them successful drug candidates [1]. Thought through formulations that protect the drugs and which are able to direct them to the destined tissue are therefore required. Nanoscale drug delivery systems (DDS) are one way to proceed [2–5]. The use of nanoscale DDS opens novel ways of drug therapy by allowing drug targeting and release at the desired area at a desired time point. This can be achieved by incorporation of drugs into (biodegradable) polymeric nanoparticles, liposomes, solid lipid nanoparticles (SLN), surfactant- or lipid-modified hydrogels or complex non-viral gene transfection systems. The affinity towards the site of action (bioadhesion) can be further enhanced by modification of the DDS' surface with target-seeking moieties, such as lectins, antibodies, peptides, carbohydrates or invasion factors.

With these very formidable requirements in mind, the thorough characterisation of nanoscale DDS during development and the in-process-control during production are of utmost importance. In this rapidly growing area of research, special attention has been given to the physicochemical characterisation, including the determination of the size distribution, charge density, time dependence of the drug release and analysis of the adhesive properties. Moreover, investigating and visualising the DDS' surface morphology can help gaining knowledge that ultimately will allow a deeper understanding of physical, chemical and biological phenomena unique to nanoscale entities.

Light microscopy (LM) has been and still is one of the fundamental techniques for the visualisation of drug carrier systems

* Corresponding author. Department of Pharmaceutical Technology and Biopharmacy, Philipps Universität Marburg, Ketzerbach 63, D-35032 Marburg, Germany. Tel.: +49 6421 282 5881; fax: +49 6421 282 7016.
*E-mail address:* ubakowsky@aol.com (U. Bakowsky).

0939-6411/$ - see front matter © 2009 Elsevier B.V. All rights reserved.
doi:10.1016/j.ejpb.2009.09.005

down to the micrometer range and allows investigation of two-dimensional features in the optical plane (*x*–*y*-plane) of the microscope, but determination of the *z*-position is hardly achievable. Even with sophisticated LM techniques such as confocal laser scanning microscopy (CLSM), the resolution that can be achieved is limited to approximately one micrometer by the Nyquist relation.

Developed in the 1940s, a widely used instrument for the investigation of surface morphology is the scanning electron microscope (SEM) [6]. However, by this technique only the near surface of samples can be visualised and drawing conclusions about the optical properties of an object is virtually impossible. Similar to light microscopic analysis, SEM only measures in the *x*- and *y*-dimensions of a sample and insight into the *z*-direction cannot be obtained directly. With today's general purpose SEM, resolution is limited to approximately 5 nm. However, this resolution can only be achieved under vacuum conditions. Moreover, a rather laborious sample preparation is required for SEM, including steps such as freeze drying, staining or metal coating. Both the sample preparation and the vacuum treatment can result in artefacts, and the structure that is ultimately depicted might be very different from its original condition. Novel techniques that permit imaging under ambient conditions like environmental scanning electron microscopy (ESEM) have become available, but this gentler method comes at the expense of a significantly reduced resolution [7].

The introduction of scanning probe microscopy (SPM) has revolutionised our ability to characterise small objects [8,9]. SPM allows the visualisation of samples with sub-nanometre resolution in three dimensions, in ambient air or under submerged conditions. A kindred to all SPM techniques is a probe scanning across the sample surface. The position of the probe relatively to the sample is monitored and held constant by a feedback loop. The first microscope in this family was the scanning tunnelling microscope (STM) [10]. Its development in 1981 earned its inventors, Gerd Binnig and Heinrich Rohrer, the Nobel Prize in Physics in 1986. As a prerequisite for STM, a conductive sample surface is needed, because the method relies on the detection of electric currents of tunnelling electrons of the sample surface. Unfortunately, few biological surfaces are sufficiently conductive or rigid enough to be examined directly with STM. At present, non-conductive surfaces can be examined in two ways: (1) sufficiently thin molecular layers attached to conductive substrates so that tunnelling can occur through the molecules or (2) coating or replicating non-conductive surfaces with metal layers so as to make them conductive, then imaging with the STM [11].

Overcoming this problem, Scanning Force Microscopy (also called atomic force microscopy; AFM) uses the deflection of a fine leaf spring, the AFM cantilever, for the *z*-axis feedback [12]. This enables investigating samples without the need of being considerate of the electric conductivity and stiffness. With AFM, it is possible to visualise biological as well as inorganic samples in ambient environments or submersed in liquids, permitting also the investigation of artificial membranes [13–16,24] or living cells [17–23] in their natural environment. Due to its broad applicability, AFM rapidly evolved from a mere physical microscopy technique to one of the standard methods in life sciences. In drug delivery research, AFM has already been used in pharmacological settings [25,26] as well as studies of drug particles [27–31,50], drug polymorphisms [32–36], drug/DNA interactions [37,38], pharmaceutical excipients [39,40], molecular forces and ligand/receptor interactions [41–45] and nanoscale DDS [8]. Other SPM techniques are scanning optical nearfield microscopy (SNOM) [46] and scanning thermal microscopy (SThM) [47,48].

This review aims to highlight some of the scope and advantages of one the SPM techniques, atomic force microscopy (AFM), in the characterisation of novel nanoscale DDS.

## 2. Atomic force microscopy

### 2.1. The principle of AFM

A schematic of an AFM set-up is shown in Fig. 1. The main element is the sensor, a pyramidal tip attached to a 100–400 μm long cantilever, which is in contact with the sample surface. Cantilever and tip are often made of silicon or silicon nitride, because these materials allow relatively cheap mass production using semi-conductor technology. The geometry of the apex of the tip is representing one of the key parameters determining the resolution. Highest resolutions can be achieved with a tip that ends in a single

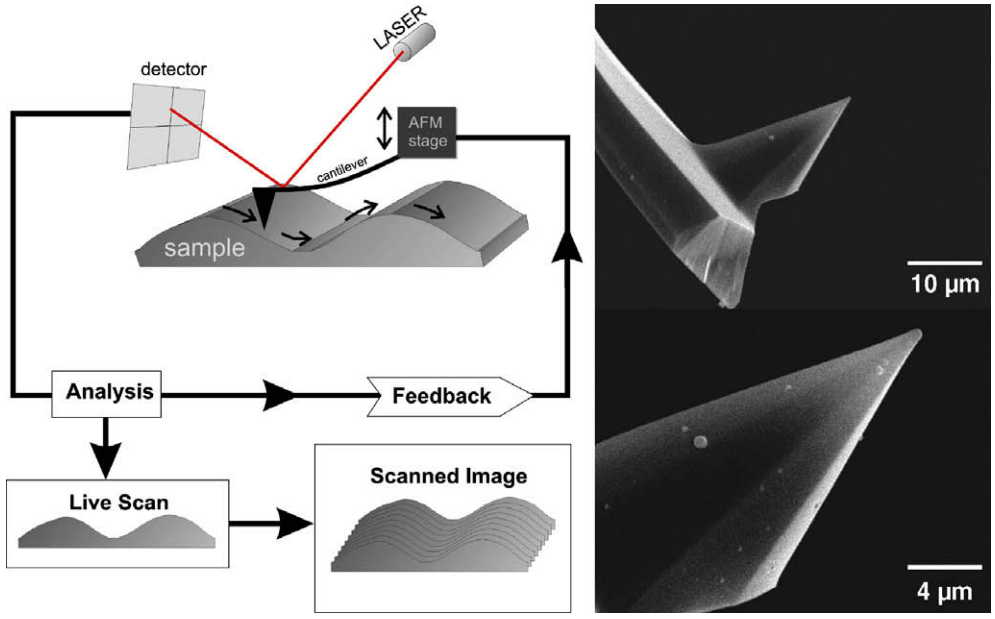


**Fig. 1.** Schematic set-up of an atomic force microscope. The cantilever/tip system is the "heart" of the AFM and determines the resolution and the quality of the measurements. Typical sharp cantilever/tip system for the use in intermitted contact mode (NSC 16, microMASH, Oelsnitz, Germany).

atom. The cantilever is a system comparable to a stylus profilometer, with the three-dimensional movement of the AFM tip relative to the sample being obtained by piezoelectric crystals. This set-up allows for positioning of the AFM tip with a precision of approximately 1 nm in *x*-, *y*- and *z*-directions.

When the AFM tip is engaging a surface, the cantilever is bending due to forces between tip and sample. This deflection, which is proportional to the force applied to the sample, is either used to directly visualise a surface topography or used as input for the feedback loop controlling the *z*-position of the AFM.

Several different techniques exist to quantify this deflection [49], but using an optical sensor is the most common one, with a laser beam being reflected from the backside of the cantilever onto a position-sensitive light detector. Since the position of the laser spot on the detector changes in correlation with the degree of bending of the AFM cantilever, the latter can be calculated accordingly.

### 2.2. Techniques in AFM

A number of different operation modes exist in AFM, such as contact AFM, intermittent contact AFM (IC-AFM or Tapping™ AFM), non-contact AFM, lateral force microscopy (LFM, see e.g. [50]), magnetic force microscopy (MFM, see e.g. [51]), magnetic AC mode force microscopy (MAC mode™ AFM, see e.g. [52]), electric force microscopy (EFM, see e.g. [53]), scanning capacitance microscopy (SCM) and atomic force spectroscopy (AFS). These techniques primarily differ in the type of interaction between the tip and the sample, but also in the way the tip is moved across the surface. The most relevant techniques for nanopharmaceutical applications are contact AFM, intermittent contact AFM, including phase imaging, and AFS. In the following, these techniques will be described in more detail.

### 2.3. Contact mode AFM

In constant height contact mode AFM, the tip is permanently engaged with the sample surface causing the cantilever to deflect. While the tip is scanning across the surface, the degree of deflection of the tip is recorded to gain information about the sample topography (Fig. 1). As the force applied to the sample is proportional to the cantilever's deflection, it is obvious that protruding features on a sample undergo high physical stresses when scanned by the tip. Pressures in the GPa range may occur during this scanning process [54]. To limit the exposure of the sample to such high forces, the constant force contact mode was developed. Here, while the tip is scanning across the sample surface, the detector signal is monitored and used as feedback to change the height of the AFM stage in a way that the deflection of the cantilever remains constant. The movement and height of the AFM stage then become a direct indicator of the surface topography. Both contact modes offer the highest resolution, allowing e.g., the visualisation of the electronic configuration of single atoms [55]. However, the use of contact mode AFM is limited to relatively hard samples, since during scanning, strong lateral forces occur, which can easily damage the sample surface.

### 2.4. Intermittent contact AFM

Intermittent contact AFM (IC-AFM) or Tapping™ AFM overcomes these previously mentioned limitations by minimising lateral forces applied to the sample. This is achieved by a "tapping" tip-sample contact which only lasts for fractions of a second (in the nanosecond range). In IC-AFM mode, the cantilever oscillation is excited by a piezoelectric crystal oscillating with a frequency close to the resonance frequency of the cantilever. When the tip interacts with the sample at its low point, a damping of oscillation can be observed (Fig. 2, blue line). This damping is used as input for the feedback loop. The height of the AFM stage is then adjusted accordingly, keeping the damping at constant rate. The topography of the sample can be extracted from the up- and downwards movements of the AFM stage as it scans across the sample (comparable to the constant force contact mode). Due to the marginal forces applied, IC-AFM allows to investigate very soft samples such as living cells [17–20,56], biomembranes [24] or liposomes [57–61].

### 2.5. Phase imaging

The contrast of an atomic force micrograph generally depends on the mechanical properties of the surface and the probe, for instance, the adhesiveness and elasticity. To produce a sharp image of the surface topography, the sample material has to be relatively rigid compared to the probe. As the material becomes softer, the image obtained will become more influenced by the elastic properties of the surface. In extreme cases, the tip–surface interaction can cause damage or displacement of the sample.

Phase imaging, a technique closely related to IC-AFM, allows observing surface properties beyond mere topography. During scanning in IC-AFM, the damping of the oscillation results in a loss of oscillation energy in the cantilever due to energy transfer to the sample. In addition to the lower amplitude, this also results in a phase shift of the oscillation of the cantilever. As this phase shift is a function of energy absorbancy of the sample material, it is idiosyncratic for stiff or soft materials [62], or more precisely, materials with high and low energy absorbencies [63] (see Fig. 2, red and blue line). This allows analysing the distribution of different materials or phases within the sample, for example, phase separation within lipids [64] or drug distribution within nanoparticles [31].

### 2.6. Force spectroscopy

AFM can also be used to measure forces between the tip and the sample surface and hence can used to generate force-distance curves [54]. A variety of forces can be detected. These include Coulomb forces, van der Waals forces, electrostatic forces or specific forces between ligand and receptor pairs [41–45]. As described above, the principle of AFM relies on the determination of forces occurring between the AFM tip and the sample surface. Therefore, this force determination can be used not only in a feedback loop for imaging, but also as an indicator for the intensity of interaction between sample and tip. The benefit of atomic force spectroscopy (AFS) over other techniques like the stylus profilometer is the high lateral positioning of the probe, allowing the observation of the behaviour of the sample at nanoscale resolution and the high force sensitivity, being able to record forces down to the pN range.

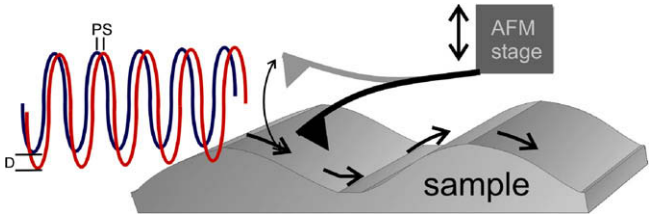


**Fig. 2.** Tapping mode AFM: cantilever oscillates with its resonance frequency (red). When brought into contact with the sample, a damping (D) of the lower amplitude as well as a phase shift (PS) are observed (blue). (For interpretation of the references to colour in this figure legend, the reader is referred to the web version of this article.)

The majority of AFS methods can be divided into two different approaches, whereas the tip either impresses the sample or the tip is retracted from the sample. From the impressing experiments, information of the (visco-)elastic behaviour of samples during deformation can be drawn, which can be used to investigate the stability and ageing of nanomaterials [65]. In retraction experiments, the adhesion between sample and tip is probed. Adhesion experiments can be performed to determine unspecific adhesion between a sample and the tip material or, after modification of the tip, to determine the interaction between a receptor and its ligand [66].

## 3. Substrates, sample preparation and probes for atomic force microscopy

### 3.1. Substrates

A meticulous sample preparation and selection of the best-suited substrate for each sample are crucial factors for high resolution and artefact-free AFM. It is paramount that the substrate is plane, and the surface roughness is substantially less than the size of objects under investigation. Substrate materials that have been successfully used in SFM include freshly cleaned surfaces of highly oriented pyrolytic graphite (HOPG), mica, evaporated or single crystal gold, silicon wafers as known from the production of electronic chips and glass slides. These surfaces can be further modified by chemical reactions in order to change their hydrophobicity, charge and charge density, the surface ion concentration and other parameters [67–72].

It also is important that the interaction forces between the sample and the substrate surface are not too strong. Otherwise, the morphology of the sample might be changed dramatically during sample preparation. On the other hand, the interaction has to be strong enough to prevent displacement of the sample during the scanning process. Hydrophilic surfaces such as mica and chemically modified mica are preferable for the examination of biological samples, because the hydrophilicity will reduce the contact angle of the wetting fluid that covers both sample and surface [49,71,73–80]. In addition, the use of silicon wafers as substrates for DNA, DNA complexes or lipids has been described [24,25,81,82]. For an extensive overview of suitable substrate materials, the reader is referred to Morris et al. [83], Meyer and Heinzelmann [49] and Marti et al. [80].

### 3.2. Sample preparation

Various methods are available for sample preparation. A very convenient procedure involves dissolving or suspending the sample material in water or buffer. A few microlitres of this solution/suspension are then pipetted onto the substrate and left for drying by exposed to air [22,29,31,35,42,45,69–71,77,81]. This method sometimes generates artefacts, especially, when the organisation and distribution of the molecules within the sample are dependent on their concentration, osmolarity, spreading of the droplet or time. To simply rehydrate the dried sample before the measurement is therefore not advisable. Instead, artefacts may be introduced due to structural changes during the rehydration process. These problems can be overcome by using the self-assembly technique for sample preparation: the substrate material is placed into the sample solution, and the sample molecules are allowed to adsorb under equilibrium conditions [82]. These adsorbed layers are usually very stable, and the sample can be kept under submersed conditions to avoid dehydration during preparation and measurement, and purpose-built fluid chambers are commercially available for some scanning force microscopes. An advantage of these fluid chambers is the possibility to change the environment that surrounds the sample during or in between measurements without the need of removing the sample. This might be necessary when investigation specimens such as amphiphilic molecules which require to be constantly submersed. Other preparation methods have been previously described by Thundat et al. [69–71] and Muller et al. [84].

### 3.3. Cantilever-tip systems

A key factor for high resolution imaging is the AFM tip, particularly, its geometry, radius and chemical composition. Hence, an appropriate choice of tip in conjunction with the sample and the scope of the experiment in terms of resolution requirements are essential. The main limiting factor concerning the maximum resolution of an AFM is the radius of the apex of the tip. Features in the size range of the tip are visualised distortedly and broadened, smaller features may not even be visible at all. There exist several deconvolution methods which allow to mathematically subtract the so-called tip-effect, but this is only possible to a certain extent [85]. For very high (i.e., atomic) resolution, special probes – so-called supertips – are commercially available. These are also well suited for lateral force measurements or point force measurements (see Fig. 1). AFM tips are usually manufactured from materials like silicon or silicon nitride. However, diamond, carbon or single crystals of minerals have been employed for select special applications (http://www.jpk.com/index.2.html). The most frequently used method for preparation of these probes is the microfabrication-etching technique. With this technique, the cantilever/probe systems are etched from oxidised silicon wafers using photographic masks to define the shape of the cantilever. This results in tips with a radius of less than 30 nm. Supertips can been obtained by the controlled growth of carbon filaments on the end of pyramidal $Si_3N_4$ tips [86]. The tips produced by these methods can be further surface modified yielding well-defined sensor systems for the characterisation of mechanical, elastic and chemical properties of samples at nano-resolution. Nanosensors can, for example, be created by covalent binding of moieties such as lipids, DNA, proteins or antibodies to the probe surface based upon a great variety of chemical reactions [87].

## 4. Use of AFM for the characterisation of nanoscale drug delivery systems

### 4.1. Nanoparticles

#### 4.1.1. In-process control of nanoparticle formation

The events involved in nanoparticle (NP) formation are not very well understood, partly because they are very challenging to follow.

Gu et al. [88] investigated the self-assembly of dendrimer–platinum composite NP using TEM and AFM. They found that dendrimer particles without a Pt core showed decreased heights when imaged using AFM, although TEM measurements did not show any differences in particle diameters (albeit the presence or absence of the Pt cores could be measured), suggesting that dendrimers formed two-dimensional structures on the support surface. When Pt–dendrimer complexation was prematurely terminated, a bimodal height distribution was found, and AFM images and feature height distributions showed evidence of arrested precipitation of Pt colloids, which led the authors to the conclusion of an existing correlation between Pt loading and particle height [88].

In another study, Oliva et al. [89] monitored the formation of drug-loaded nanoparticles via a self-assembly process. By mixing of solutions of carrageenan and dexchlorpheniramine maleate, an

encapsulation of the model drug into nanoparticulate structures was achieved. At an early stage, carrageenan fibrils were observed which had disappeared after 10 h of incubation, and the topographical evolution of the NP was monitored to completion, after approximately 17 h.

Moughton et al. [90] described the preparation of hollow nanocapsules by self-assembly of an amphiphilic diblock-polymer, in which hydrophilic and hydrophobic blocks were connected by a bivalent linker. After cleavage of the linker, core and shell of these micelles were disconnected from each other. By dissolution of the core, hollow nanocapsules were prepared. Specimens visualised with AFM after the cleavage step could clearly show the inner core surrounded by a corona of shell polymer, which was no longer connected to the core. As molecular organisation at the sub-nanometre scale is a very fast and elusive process, these two examples clearly show the superiority of AFM for such tasks. By AFM, it is possible to observe the sophisticated mechanisms of NP assembly *in situ*. Other microscopic methods are lacking either the necessary resolution (e.g., LM) or the possibility to measure in liquids (e.g., TEM) rendering them useless for this task.

#### 4.1.2. Measurements of nanoparticle size

The physical characteristics and morphology (i.e., size, shape, structure and integrity) of DDS directly impact on their efficiency *in vitro* and *in vivo* and need therefore to be characterised extensively. Particle size is one of the most important factors of any particulate system for pharmaceutical use. From issues of manufacturability of a dosage form to suitability for specific application routes, all depends on particle size [91–94]. Several techniques are used to determine particle sizes depending on the size range (for a review on particle size determination techniques see e.g. [95]). For nanoscale DDS, dynamic light scattering (DLS), TEM, SEM and AFM are commonly employed. Due to its principle of measurement, DLS is only capable of giving information about the volumetric mean diameter of a great number of particles, but results on the real size distribution are rather difficult to obtain. For a precise determination of single particle dimensions, microscopic techniques are required. Here, AFM often outperforms EM techniques; it is quicker, does not require a specific sample preparation and can be performed on submersed particles. Artefacts from dehydration or deposition of auxiliary materials (e.g., salts or surfactants) can, therefore, be avoided as well as coating or staining as necessary for EM. Lastly, the powerful electron beam can melt or sinter polymeric materials rendering EM useless for the investigation of certain materials.

With the high precision in lateral and vertical positioning of the AFM tip, in principle it is possible to determine the dimensions of nanoparticles with high accuracy. Nonetheless, factors such as elastic behaviour of the sample [88] and the support as well as non-linear behaviour of the positioning piezo elements can decrease accuracy.

Generally, prerequisite for the exact determination of NP dimensions is a rigid and even sample support. However, the determination of NP dimensions on rough and elastic surfaces like cellular membranes was suggested by Oikawa et al. [96]. They developed a method to calculate the size of metal NP from the curvature recorded by AFM.

Roe et al. [97] determined the height of immobilised latex NP using AFM. They were able to show that on the edge of a NP monolayer the height of individual NP could be determined with an error less than 2%. This seminal work corroborated the applicability of AFM to determine NP sizes.

When NPs are visualised using AFM, the observed width/height ratio is always greater than 1. This is due to the width of the AFM tip and the flattening process of particulate objects when adsorbed to a surface. The broadening effect caused by the AFM-tip geometry was first shown by Lacava et al. [98] who compared size distributions of magnetic NP of sizes below 10 nm by AFM and TEM. With AFM-tip radii 10 times as big as the diameter of the NP, they found a smaller mean diameter (80%). In addition, the accuracy decreased, as evident by an increased standard deviation (115%). This again underlines the importance of choosing the proper tip in order to obtain meaningful data.

To minimise these interfacial phenomena, De Assis et al. [99] used glutaraldehyde as a crosslinker stabilising NP made from Poly(Lactic Acid) (PLA). They found that the width/height ratio decreased one order of magnitude with the use of the crosslinker. They also investigated the stability of NP following adsorption onto mica. Their results confirmed that NP continues to aggregate after sample preparation, which again could be avoided by glutaraldehyde fixation.

Wooley [100] described the use of shell-crosslinked core–shell particles prepared from AB-blockpolymers, consisting of a hydrophobic and a hydrophilic block, representing the core and the shell of the formed NP. The systems were investigated before and after crosslinking of the shell. Before crosslinking, NP showed a tendency to spread on the mica support, due to their low stability and high fluidity (the phase transition temperature (TG) of the core polymer block was −71 °C). However, after crosslinking, NP kept their round shape and their heights were consistent with TEM size measurements. The same group showed in another publication [101] that crosslinked core–shell particles still flatten on a mica surface, whereas subsequent crosslinking of the core domain (in addition to the initial shell crosslinking) increased morphological stability further.

Zhang et al. [102] investigated core–shell NP consisting of the copolymer poly(ε-caprolactone)-b-poly(acrylic acid) (PCL-b-PAA). The two step preparation (1. formation of polymeric micelles; 2. crosslinking of the micellar shell) led to NP with a crystalline, biodegradable core within a crosslinked hydrophilic shell. By AFM, they found that a higher degree of crosslinking stabilised the three-dimensional structure of these NP. The hydrolysis of the core was also followed using AFM under immersed conditions. Over time, the NP decreased in height but maintained their round shape.

Paik et al. [103] investigated the elastic behaviour of poly(propylene) NP as a function of loading force, indentation depth and diameter. They found that NP size had an impact on the measured elasticity. Since NP size has correlating influences on the TG of the investigated systems, the authors claimed that size dependent crystallinity of the polymer within the NP may be the reason for the different elastic behaviour.

#### 4.1.3. Measurements of nanoparticle stability, release and degradation

The storage stability of pharmaceutical NP is one of the factors that ultimately decide over the fate and success of the system. Changes in degree of dispersion are easily overlooked due to the small size and large number of individual particles (Fig. 3). If the aggregated fraction is less than 10% of all particles, DLS does not have the ability to determine the multimodal size distribution [104]. This limitation does not apply for AFM, hence, it is easily possible to differentiate between single, aggregated and fused particles. This potential advantage of AFM over DLS was shown by Montasser et al. [105] who reported that a bimodal size distribution was observable with AFM which could not be resolved by DLS techniques. Since, AFM has been used in several studies to measure the degree of aggregation or to investigate the structure of agglomerates [106–111].

Dailey et al. [109] investigated the stability of NP for pulmonary delivery during the nebulisation process. They found that a higher content of the stabiliser, carboxymethylcellulose, prevented formation of aggregates. The impact of freeze drying on the resuspendability of PolyEthylenGlycol (PEG)-PLA NP was studied by

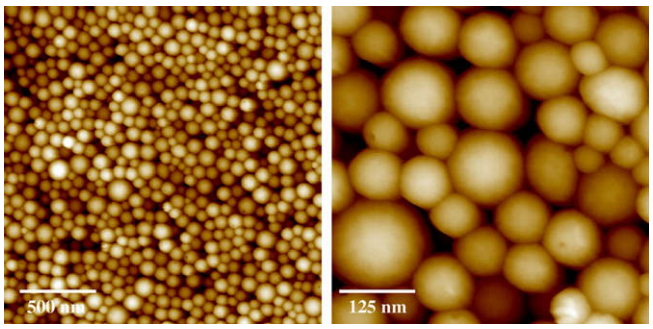


**Fig. 3.** AFM images of biodegradable 125-nm-sized PLGA/chitosan nanoparticles prepared according to M.N.V.R. Kumar [111], visualised with TappingMode™ (Digital Instruments, Nanoscope IV Bioscope) in air.

Görner et al. [112]. Their initial data showed that lidocaine-loaded NP did not readily resuspend after freeze drying. By AFM, they could ascertain that drug-loaded NP had fused into larger structures, whereas unloaded NP remained mostly unaffected.

Controlled aggregation and fusion of nanoparticles into *in situ*-forming depots were investigated by Packhäuser and Kissel [107], when studying ion-mediated aggregation of positively charged polymer NP loaded with insulin. AFM analysis showed that at low salt concentrations, discreet NPs were found, whereas in isotonic conditions NP had fused into a porous gel.

Weiss et al. [65] studied the stability and degradation behaviour of Poly(Lactic-co-Glycolic Acid) (PLGA) NP which had been stored for up to 15 weeks. During that period, no NP aggregation was observed by AFM. A nanoporous surface developed over time, as the PLGA degraded. Phase imaging showed significant changes in NP elasticity. After 15 weeks, pore depths had decreased indicative of a fluidising effect of short chain length PLGA that had started to degrade.

Silica–polymer composite NPs containing a silica core surrounded by a poly-N-isopropylacrylamide polymer were investigated by Yuan et al. [113]. When AFM samples were prepared at room temperature, the hydrophilic shell detached from the NP surface, forming a polymer film with the core particles embedded on the sample support. However, when samples were prepared at elevated temperatures, the polymer did not detach and instead large core–shell NP were obtained.

#### 4.1.4. Investigations of nanoparticle surface modifications

Due to its high resolution, AFM is also very well suited for imaging surface features of nanoparticulate systems. Initial studies in this area were carried out by Ramesh et al. [114] when attaching 20-nm nickel nanocrystals to 200-nm amorphous silica NP and subsequently imaging the surface topography of the aggregates. As complementary technique, TEM was used. For these electron dense materials, TEM could achieve very good results. However, when using polymeric systems instead of metals, AFM has a clear advantage over electron microscopy, as shown by Mu et al. [115] when investigating the surface morphology of polymeric particles using AFM and SEM. SEM images showed a relatively smooth surface, whereas AFM revealed nano-sized cracks and invaginations on the particle surface. These surface features could be used to explain the rate of drug release from the particles. In a similar study, Feng et al. [116] investigated the morphology of NP loaded with paclitaxel reporting nanoporous topography, which again was consistent with the observed drug release profile.

Wang et al. [117] used 100-nm silica NP coated with bovine serum albumin (BSA) to prepare micro arrays. On these particles, BSA molecules could clearly be visualised using phase imaging AFM. This clearly shows the ability of AFM to identify protein layers (which have a molecular volume of about 20 $nm^3$ [118]) on extensively curved materials such as nanoparticles. A related study was conducted by Cai et al. [119]. Here, AFM studies were performed on NP consisting of a blend of PLGA and poly(styrene-co-4-styrenesulfonate). These NPs were loaded with lysozyme, a positively charged protein. Using TEM and AFM as complementary methods, they were able to display the protein absorbed to the NP surface. In TEM images, a corona of proteins surrounding the NP core was shown, whereas in AFM investigations the protein-coated NP showed a significantly higher roughness compared to unmodified NP.

In the study of Schäfer and co-workers [120], inconsistencies in the lipid coating of chitosan–PLGA NP were visualised as 4–5 nm steps on the surface of the particles by AFM, a value similar to the height of a DiPalmitoylPhosphatidylCholine (DPPC) bilayer. It should be noted that TEM experiments were unable to show this subtle changes in surface topography (unpublished data).

AFM phase imaging can also be used to determine drug distribution within a polymeric nanocomplex. Simon et al. [31] reported that single NP investigated in phase mode showed an uneven distribution of surface behaviour (Fig. 4). The authors concluded that this was due to a heterogeneous distribution of insulin within the complexes. Phase imaging on crystals of insulin with Neutral Protamine Hagedorn (NPH) has also been investigated by Yip et al. [121].

### 4.2. Liposomes

Liposomes are extremely versatile DDS allowing the incorporation of hydrophilic, hydrophobic or amphiphilic substances combined with a hereditary biocompatibility comprising endogenous phospholipids. In addition, liposomal properties such as charge, diameter, membrane permeability and loading capacity can easily be modified [59,60,122–131]. Liposomes can reduce the toxic side effects, target drugs to specific tissues and modulate the pharmacokinetics of liposome-associated and encapsulated drugs, making them valuable systems for intravenous, topical and pulmonary drug delivery [124,125]. Hence, liposomes have been described for the delivery of enzymes [126], anticancer drugs [122,123,128,129,132] anti-microbial drugs [124] and many other compounds.

In addition to studies of solid nanoscale DDS (see above), AFM can be used for morphological investigations and interaction stud-

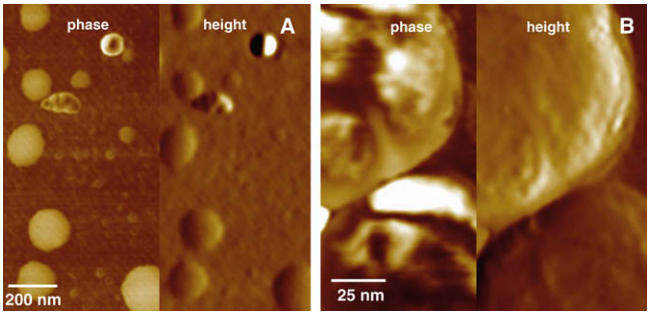


**Fig. 4.** Phase contrast imaging. With the AFM the material properties can be visualised. (A) PLGA/chitosan/dexamethasone nanoparticle, the drug is homogeneously distributed within the nanoparticles, the particles show the same bright colour (unpublished results), (B) poly[(vinyl-3-(diethylamino)-propylcarbamate*co*-(vinyl acetate)-*co*-(vinyl alcohol)]-graft-poly(L-lactic acid)/insulin nanoparticles (size 200 nm), the insulin is inhomogeneously distributed (bright areas) according to [31]. Left phase contrast image/right height image, dark areas are softer then bright areas. All images visualised with TappingMode™ (Digital Instruments, Nanoscope IV Bioscope) under ambient conditions. (For interpretation of the references to colour in this figure legend, the reader is referred to the web version of this paper.)

ies of lipid-based systems as well, albeit a higher degree of spreading on the substrate is usually observed, due to their fluidic nature [2,9,131]. The concept of sterical stabilisation has been initially developed for long circulation liposomes but has also been adopted to increase liposome stability in, e.g., lung surfactant layers [60]. Moreover, it was reported by Bakowsky et al. that the addition of PEG to the lipid mixture prevented liposome spreading on surfaces in a concentration-dependant manner [59]. The reduced spreading allows studying lipid vesicle morphologies in a closer-to-life scenario as they appear rounded in atomic force micrographs compared to non-PEGylated systems.

Complement activation is an important step in the acceleration of liposome clearance. Carmo et al. [133] characterised complement activation of conventional and long-circulating pH-sensitive and non-pH-sensitive liposomes using a haemolytic assay in rat serum and AFM. The AFM images showed that non-PEGylated, pH-sensitive liposomes were prone to vesicle aggregation which activated the complement system.

In order to achieve active drug targeting, specific ligands can easily be attached to the liposome surface, for instance, antibodies, resulting in so-called immunoliposomes. If the surface-bound ligand is of suitable size, the successful conjugation can be visualised by means of AFM. Bendas et al. [134] developed long-circulating immunoliposomes, which combined sterical stabilisation with a superior targetability, introducing a new methodology for attaching monoclonal antibodies directly to the distal ends of liposome-grafted PEG chains. The different surface morphologies in dependence on the coating strategy were visualised by AFM. The antibodies could be depicted with a resolution of 0.2 nm in aqueous solution. Similarly, Anabousi et al. [130] suggested to use AFM (and TEM) for the visual assessment and quantification of the surface modification with a serum protein, transferrin. Having the visual information of the actual localisation of the ligand at hand is arguably a clear advantage to the commonly used protein quantification assays which are unable to differentiate between encapsulated, conjugated and surface-absorbed ligands.

The rigidity of liposomes is one of the key factors affecting release profiles of encapsulated drug and blood circulation time. Measurements of liposome rigidity in buffer solutions were performed by Nakano et al. [135] using tapping mode AFM. Ramachandran et al. [123] had previously reported that encapsulation of cisplatin into liposomes resulted in an approximately 100% increase in rigidity compared to liposomes without cisplatin. Thus, AFM force-dissection and stiffness measurements can be employed as methods to investigate the encapsulation efficiency of certain drugs into lipid vesicles.

Vesicle size and shape as well as rate of drug release are strongly dependent on the phase behaviour of the lipids comprising the systems. Sakai et al. [136] analysed the structural transition of L-α-DPPC liposomes caused by the addition of small amounts of stearylamine (SA). Colloid probe AFM revealed that the addition of SA resulted in inter-film electrosteric repulsion. This repulsive interaction caused a significant increase in the inter-bilayer distance, and hence affected the shape of the vesicle. In a related study, Liang et al. [137] showed that the addition of cholesterol to egg yolk phosphatidylcholine (EggPC) vesicles also influenced the mechanical properties of the lipid bilayers. The elastic properties evaluated from conventional force measurements in contact mode showed that Young's modulus of cholesterol-modified vesicles increased several-fold compared to plain EggPC vesicles.

Ruozi et al. [138] studied the influence of the lipid composition on the physical stability of liposomes during their storage using AFM and photon correlation spectroscopy (PCS). After 7 months of storage, the average sizes of the different liposomes evaluated using the two techniques were comparable. However, while PCS could only measure the vesicle size and polydispersity of the size distribution, AFM confirmed that the increase in size and size distribution were not the result of vesicle aggregation, but of vesicle fusion.

Berquand et al. [139] used AFM to characterise the influence of the macrolide antibiotic, azithromycin, on the molecular organisation of DPPC:DiOleoylPhosphatidylCholine (DOPC), DiPalmitoylPhosphoEthanolamine (DPPE):DOPC, SphingoMyelin (SM):DOPC and SM:Chol:DOPC lipid vesicles, as well as the effect of azithromycin on membrane fluidity and permeability. *In situ* AFM images revealed that azithromycin leads to erosion and disappearance of DPPC and DPPE gel domains, whereas no effect was noted on SM and SM:chol domains. Although azithromycin did not alter the permeability of any of the lipid vesicles, it increased the fluidity at the hydrophilic/hydrophobic interface in DPPC:DOPC and DPPE:DOPC membrane models. This study showed once more the capability of AFM methods to characterise drug–membrane interactions. These results were later confirmed in a further study [140].

### 4.3. Non-viral gene transfection systems

Arguably, the biopolymers most frequently investigated by AFM are nucleic acid derivatives (in the context of gene therapy and gene/siRNA delivery). Among these are complexes of DNA, siRNA, DNAzyme and ribozyme with other biomolecules, as well as fully synthetic gene transfection or inhibition systems. The latter include transfection complexes based on positively charged lipids, liposomes, proteins, polymers and nanoparticles. AFM has been used to study the influence of polymer chain length, molecular weight, charge density and environment on the size, shape, charge and stability of such complexes. The first high resolution image of nucleic acids was reported by Hansma et al. [73–75], after they adsorbed a short synthetic DNA onto a positively charged mica substrate. With this method, the visualisation of single base pairs could be achieved. An example of such an atomic force micrograph, showing a resolution at the molecular level, is given in Fig. 5.

The main body of investigations on non-viral gene transfection systems are carried out to visualise the size, shape and organisation of complexes of lipid/DNA (lipoplexes) [81,82,110,141, 142, 91,143,144] or polymer/DNA (polyplexes) [110,111,145–151,92, 152,153].

Marty et al. [142] investigated the complexation of calf-thymus DNA with cholesterol, DiOleoylTrimethylAmmonium-Propane (DOTAP), DimethylDioctAdecylammonium Bromide (DDAB) and DOPE under physiological condition. Almofti et al. [91] showed by AFM that lipoplexes formed from extensively fused and apparently homogeneous lipid particles encapsulating DNA. Kawaura et al. [143] showed, using lipoplexes made of cationic cholesterol derivative with different spacer arms and the helper lipid DOPE, that the complex diameters depended on the choice of cholesterol derivative. Kneuer et al. [110] compared various polycationic vehicles regarding their biophysical properties. The morphology of liposomes (DOTAP, SAINT 2) with and without helper lipid (DOPE), the polymer, polyethyleneimine (PEI) and cationic nanoparticles (Si26H, PLGA/chitosan) was visualised and compared with regard to their transfection efficacy. Zhao et al. [144] used AFM for the visualisation of the lipoplexes and additionally for the characterisation of the change of membrane pore size in HER-2 cells.

However, only few studies analysed the actual formation of the complex. Oberle et al. [82] studied the interaction between a plasmid and cationic amphiphiles, so-called SAINTS, using a monolayer technique. Their data revealed a three-step mechanism of complex formation at molecular level. It could be shown that individual plasmids enwrap themselves with amphiphile molecules in a multilamellar fashion. The size of the complexes formed was depending on the supercoiled size of the plasmid, and calculations revealed that the plasmids were surrounded by 3–5 bilayers of

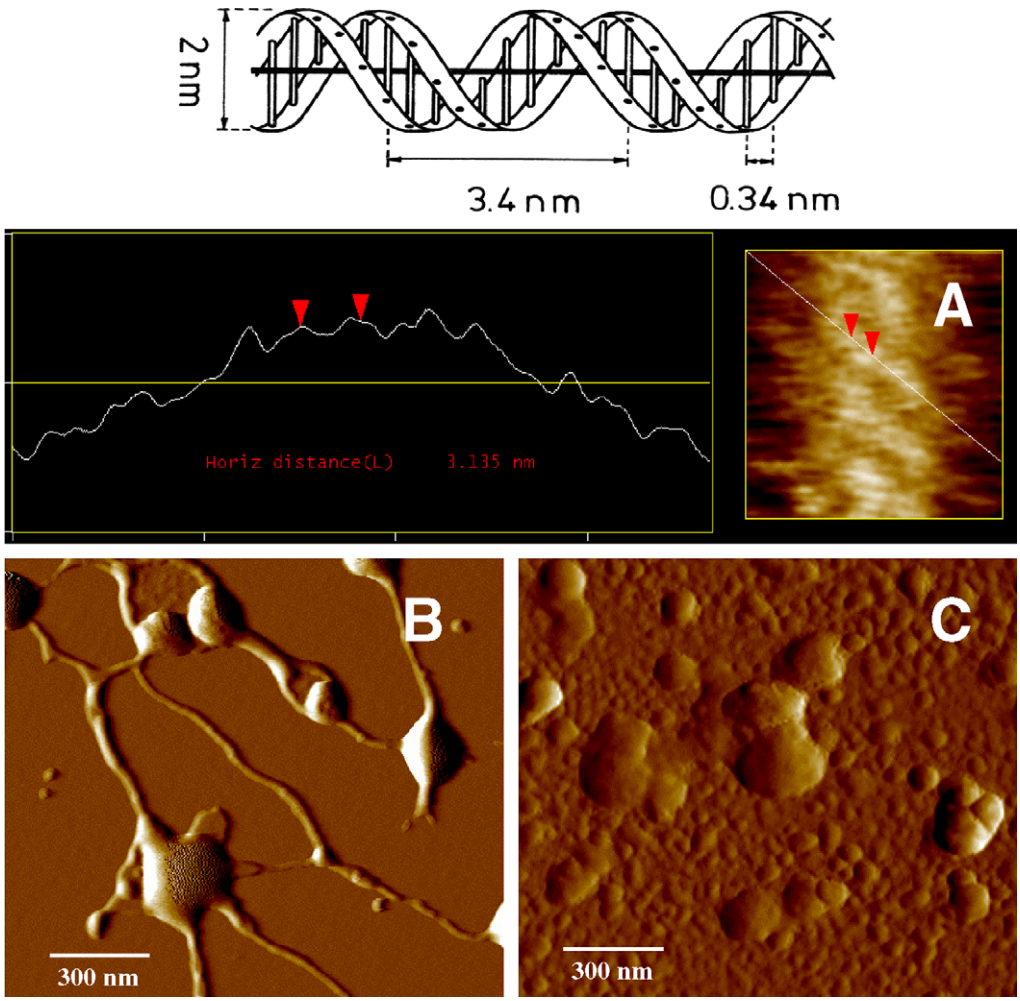


**Fig. 5.** Visualisation of the structure of DNA and gene transfection systems. (A) High resolution image (0.1 nm) of a relaxed plasmid DNA (pCMVbeta). The distances between the loops could be measured and correlate with the DNA model according to [82]. (B) The complexes (lipoplexes) shown here are the results of self-assembly of SAINT 2 and DNA (pCMVbeta). The DNA was covered by the lipid, some non-condensed plasmids could be visualised [82]. (C) Typical morphology of PEI/DNA complexes. The mean diameter of the complexes is in the range of 100–200 nm according to [92].

the amphiphiles. Additional investigations by Zuhorn et al. [81,141] showed the significance of the preference of DiOleoyl-PhosphoEthanolamine (DOPE) to adopt hexagonal phases during the mechanism of transfection.

In a study by Martin et al. [154], AFM was used to study the formation of polyamidoamine/DNA complexes in aqueous solutions. This study did show not only the structure of these complexes to be either rod-like or toroidal, but also that there is a dynamic equilibrium between these two states.

The inhibition of DNA-digestion of polyamidoamine dendrimer/DNA complexes was shown by Abdelhady et al. [155]. While naked DNA and complexes with low polymer content were not densely complexed, and therefore, DNA was prone to DNase digestion, an excess of polymer led to densely packed complexes. After incubation with DNase and subsequent disassembly of these complexes, no degradation of the plasmid was visible.

Grzelinski et al. [156] investigated the potential of low-molecular weight PEI to perform DNA transfection and siRNA gene targeting in the presence of serum. Physicochemical analysis and AFM revealed a distinct size pattern with the presence of two complex subgroups and showed that frozen PEI complexes remained stable with little increase in complex size, no changes regarding their zeta potential and cytotoxicity, and full retention of nucleic acid protection.

Pennadam et al. [157] investigated PEI grafted with poly(N-isopropylacrylamide). This thermoresponsive polymer was used to form complexes with DNA which were examined at different temperatures. AFM images revealed changes in complex structure, which were too subtle to be recognized by DLS, but confirmed fluorescence data which indicated a change in hydrophobicity, finally leading to aggregation.

Mao et al. [92] used AFM to study the effect of PEGylation on the biophysical properties of PEI–siRNA polyplexes. Particle size and stability against heparin as well as RNase digestion of different siRNA polyplexes were characterised. In a related study from the same laboratory, Neu et al. [152] generated stabilised PEI/DNA polyplexes by crosslinking PEI with biodegradable disulfide bonds. Polyplex morphology and mechanic stability were investigated using AFM and revealed no changes in the morphology of crosslinked PEI polyplexes, and indentation force measurements using AFM showed significantly increased mechanical stability of crosslinked PEI polyplexes. AFM has also been used to study the influence of polymer chain length on the size and shape of poly-L-lysine/DNA complexes [145] and to study the change in the structure of such complexes from globular to toroidal after the addition of hydrophilic PEG blocks to the polymer [146].

A study by Kleemann and co-workers [158] investigated the effect of several modifications of PEI before and after nebulization.

They found that PEG-PEI was able to strongly interact with the plasmid DNA, shelter the plasmid from DNAse digestion and stabilize the complex during nebulisation.

Chim and co-workers [151] studied Poly[2-(dimethylamino)ethyl methacrylate-b-2-methacryloyloxyethyl phosphorylcholine] (DMA-MPC) as a new vector candidate for gene therapy. They assessed the morphology of DNA complexes obtained using the diblock copolymer series DMA(x)MPC30 using TEM and submerged AFM. Both techniques indicated more compact, complex morphologies with increasing length of the cationic DMA block. However, the detailed morphology of the DMA(x)MPC30-DNA complexes observed by TEM *in vacuo* and by AFM *in situ* was different. By using TEM, the morphology of the complexes changes from loosely condensed structures to highly condensed rods, toroids and oval-shaped particles as the length of the DMA moiety increased. In contrast, morphological changes from plectonemic loops to flower-like and rectangular block-like structures, with an increase in highly condensed central regions were observed by AFM. It was suggested that the open structures observed by AFM were closer to the actual morphology as the ambient conditions during the. AFM analysis was much closer to reality.

### 4.4. Biomembranes and DDS interaction with biomembranes

The interaction of nanoscale DDS with biomembranes is one of the first steps in the absorption cascade across biological barriers like epithelia and endothelia. This intensity of the interaction is of relevance, because stronger interactions will lead to larger amounts of drug deposited in the target tissue. A strong interaction, on the other hand, may also result in membrane destabilisation, causing cellular toxicity. Measurements of DDS-membrane interactions are, therefore, of great interest in nanopharmaceutical research. Shortfalls of other microscopic techniques like the low resolution of LM or the sample preparation in EM again render AFM an important tool in this area.

Peetla et al. [159] studied the interaction of polystyrene NP with an artificial cellular model membrane. They found that NP affects the size and distribution of lipid rafts in these membranes in dependence on particle diameter and surface chemistry. The membrane interactions of cationic NP were also investigated by Leroueil et al. [160]. In their studies using AFM to assess changes in membrane morphology, they found that biological as well as artificial cationic NP could induce membrane disorders, including holes, membrane thinning and even disruption. DDS was found to be accumulated in these areas of disorder.

The influence of DDS size on membrane interaction and transport was investigated by Kanno and co-workers [161] using polystyrene nanoparticles with sizes ranging from 20 nm to 1 μm as probes. Their data suggest that 20-nm particles adsorbed in small agglomerates to the cellular membrane, while larger particles adhered non-agglomerated. They hence concluded that cellular uptake of NP is independent of size below a certain threshold when agglomeration occurs. Pan et al. [162] investigated the uptake of transferrin-conjugated quantum dots (QD) into HepG2 cells. By studying cell morphology, cellular volume and contact angle between support surface and cell body using AFM, a transferrin-induced endocytotic mechanism was revealed which lead to the formation of endosomes. The endosomal vesicles could be visualised underneath the cellular membrane by AFM as well.

The nature of biological membrane studies essentially required the presence of water rendering electron microscopic studies more or less useless for studies in this area. Light microscopic methods, on the other hand, are lacking the magnification to observe interactions of nanoscale materials with biological membranes. AFM, however, is ideally positioned for these kinds of experiments. It can be predicted that NP-modified AFM tips and simultaneous methods (e.g., AFM-Raman or AFM-fluorescence) will increase our knowledge in this specific area dramatically over the next couple of years.

## 5. Conclusions

The use of atomic force microscopy in nanopharmaceutical drug delivery research enables us to directly observe DDS without the need of cumbersome and potentially adulterating sample preparation. Nanoscale DDS can be investigated in a controlled environment without the necessity of staining or drying. Intermittent contact mode AFM allows the investigation of soft samples with minimal sample alteration; phase imaging allows to access information beyond the samples topography and also allows differentiating between different materials; force spectroscopy experiments are helping us to understand the intrinsic structure of DDS by assessing the elastic or adhesion behaviours of particles. Using AFM for DDS development hence allows us to gather information which is hardly accessible by any other experimental technique. AFM can therefore provide invaluable information about physicochemical properties which decide on the success of a potential DDS. A significant amount of work has been carried out in nanopharmaceutical research in recent years using a great variety of different techniques. AFM has already helped a lot to shed light into the area of nanoscale drug delivery and will definitely add a lot more to our understanding of the behaviour of nanoscale DDS in the time to come.

## Acknowledgements

The authors gratefully acknowledge the support of T. Kissel and A. Aigner (Philipps-University Marburg, Germany), C.-M. Lehr (Saarland University, Germany). D. Hoekstra (University of Groningen, The Netherlands) and M.N.V. Ravi Kumar (Strathclyde University, UK). This work has been funded in part by the Leopoldina Foundation BMBF 9901/8-6, DFG Forschergruppe 627 "Nanohale", DFG Forschergruppe 495 "Biohybride" and a Strategic Research Cluster Grant (07/SRC/B1154) under the National Development Plan co-funded by EU Structural Funds and Science Foundation Ireland.

## References

[1] C.A. Lipinski, Drug-like properties and the causes of poor solubility and poor permeability, J. Pharm. Tox. Meth. 44 (1) (2000) 235–249.
[2] R. Langer, Drug delivery and targeting, Nature 392 (6679) (1998) 5–10.
[3] L. Zhang, F.X. Gu, J.M. Chan, A.Z. Wang, R.S. Langer, O.C. Farokhzad, Nanoparticles in medicine: therapeutic applications and developments, J. Clin. Pharm. Ther. 83 (5) (2008) 761–769.
[4] K.S. Soppimath, T.M. Aminabhavi, A.R. Kulkarni, W.E. Rudzinski, Biodegradable polymeric nanoparticles as drug delivery devices, J. Control. Release 70 (1–2) (2001) 1–20.
[5] T.M. Allen, P.R. Cullis, Drug delivery systems: entering the mainstream, Science 303 (2004) 1818–1822.
[6] I.M. Abrams, J.W. McBain, A closed cell for electron microscopy, J. Appl. Phys. 15 (1944) 607–609.
[7] J.A. Swif, A.C. Brown, An environmental cell for the examination of wet biological specimens at atmospheric pressure by transmission scanning electron microscopy, J. Phys. E 3 (1970) 924–926.
[8] M. Davies, A. Brindley, X. Chen, M. Marlow, S.W. Doughty, I. Shrubb, C.J. Roberts, Characterization of drug particle surface energetics and Youngs modulus by atomic force microscopy and inverse gas chromatography, Pharm. Res. 22 (7) (2005) 1158–1166.
[9] Y.T. Turner, C.J. Roberts, M.C. Davies, Scanning probe microscopy in the field of drug delivery, Adv. Drug Deliv. Rev. 59 (14) (2007) 1453–1473.
[10] G. Binnig, H. Rohrer, Scanning tunnelling microscopy, Helv. Phys. Acta 55 (1982) 726–735.
[11] J.A. Zasadzinski, Scanning tunneling microscopy with applications to biological surfaces, Biotechniques 7 (2) (1989) 174–187.
[12] G. Binnig, C.F. Quate, C. Gerber, Atomic force microscope, Phys. Rev. Lett. 56 (1986) 930–933.

[13] A. Mecke, S. Uppuluri, T.M. Sassanella, D.K. Lee, A. Ramamoorthy, J.R. Baker, B.G. Orr, Direct observation of lipid bilayer disruption by poly (amidoamine) dendrimers, Chem. Phys. Lip. 132 (2004) 3–14.
[14] D. Pesen, J.H. Hoh, Micromechanical architecture of the endothelial cell cortex, Biophys. J. 88 (1) (2005) 670–679.
[15] K.J. Van Vliet, P. Hinterdorfer, Probing drug–cell interactions, Nano Today 1 (3) (2006) 18–25.
[16] E. Henderson, Imaging of living cells by atomic force microscopy, Prog. Surf. Sci. 46 (1) (1994) 39–60.
[17] R.d.S. Pereira, Detection of the absorption of glucose molecules by living cells using atomic force microscopy, FEBS Lett. 475 (1) (2000) 43–46.
[18] G.H. Dong, L. Danying, C. Weiguo, S. Yunxu, J. Lei, M. Wanyun, C. Wang, MAC mode atomic force microscopy studies of living samples, ranging from cells to fresh tissue, Ultramicroscopy 107 (4–5) (2007) 299–307.
[19] S.W. Schneider, M.E. Egan, B.P. Jena, W.B. Guggino, H. Oberleithner, J.P. Geibel, Continuous detection of extracellular ATP on living cells by using atomic force microscopy, PNAS 96 (1999) 12180–12185.
[20] S.W. Schneider, P. Pagel, C. Rotsch, T. Danker, H. Oberleithner, M. Radmacher, A. Schwab, Volume dynamics in migrating epithelial cells measured with atomic force microscopy, Pflugers Arch. Eur. J. Physiol. 439 (3) (2000) 297–303.
[21] M. Radmacher, Measuring the elastic properties of biological samples with the AFM, IEEE Eng. Med. Biol. Mag. 16 (2) (1997) 47–57.
[22] F.M. Ohnesorge, J.K. Horber, W. Haberle, C.P. Czerny, D.P. Smith, G. Binnig, AFM review study on pox viruses and living cells, Biophys. J. 73 (4) (1997) 2183–2194.
[23] P. Li, F. Yu, C. Loehbach, F. Muecklich, C.M. Lehr, U. Bakowsky, New methods of laser ablation patterning induces directional cell growth, IEEE Trans. NanoBiosci. 2 (3) (2003) 138–145.
[24] K. Christ, I. Wiedemann, U. Bakowsky, H.G. Sahl, G. Bendas, The role of lipid II in membrane binding of and pore formation by nisin analyzed by two combined biosensor techniques, Biochim. Biophys. Acta. 1768 (3) (2007) 694–704.
[25] A. Berquand, M. Mingeot-Leclercq, Y. Dufrene, Real-time imaging of drug–membrane interactions by atomic force microscopy, BBA-Biomembr. 1664 (2004) 198–205.
[26] R.d.S. Pereira, Atomic force microscopy as a novel pharmacological tool, Biochem. Pharm. 62 (8) (2001) 975–983.
[27] A. Danesh, M.C. Davies, S.J. Hinder, C.J. Roberts, S.J. Tendler, P.M. Williams, M.J. Wilkins, Surface characterization of aspirin crystal planes by dynamic chemical force microscopy, Anal. Chem. 72 (15) (2000) 3419–3422.
[28] A. Danesh, S.D. Connell, M.C. Davies, C.J. Roberts, S.J.B. Tendler, P.M. Williams, M.J. Wilkins, An in situ dissolution study of aspirin crystal planes (1 0 0) and (0 0 1) by atomic force microscopy, Pharm. Res. 18 (3) (2001) 299–303.
[29] C. Kneuer, M. Sameti, U. Bakowsky, T. Schiestel, H. Schirra, H. Schmidt, C.M. Lehr, Surface modified silica-nanoparticles can enhance transfection *in vitro*: a novel class of non-viral DNA vectors, Bioconj. Chem. 11 (6) (2000) 926–932.
[30] U. Westedt, M. Kalinowski, M. Wittmar, T. Merdan, F. Unger, J. Fuchs, S. Schaller, U. Bakowsky, T. Kissel, Poly(vinyl alcohol)-graft-poly(lactide-co-glycolide) nanoparticles for local delivery of paclitaxel for restenosis treatment, J. Control. Release 119 (1) (2007) 41–51.
[31] M. Simon, M. Wittmar, U. Bakowsky, T. Kissel, Self-assembling nanoplexes from insulin and water-soluble branched polyesters, poly[(vinyl-3-(diethylamino)-propylcarbamate-co-(vinyl acetate)-co-(vinyl alcohol)]-graft-poly(L-lactic acid): A novel carrier for transmucosal delivery of peptides, Bioconj. Chem. 15 (2004) 841–849.
[32] G.H.W. Sanders, C.J. Roberts, A. Danesh, A.J. Murray, D.M. Price, M.C. Davies, S.J.B. Tendler, M.J. Wilkins, Discrimination of polymorphic forms of a drug product by localized thermal analysis, short Communication, J. Microsc. 198 (2) (2000) 77–81.
[33] S. Ward, M. Perkins, J. Zhang, C.J. Roberts, C.E. Madden, S.Y. Luk, N. Patel, S.J. Ebbens, Identifying and mapping surface amorphous domains, Pharm. Res. 22 (7) (2005) 1195–1202.
[34] G.B. Onoa, G. Cervantes, V. Moreno, M.J. Prieto, Study of the interaction of DNA with cisplatin and other Pd(II) and Pt(II) complexes by atomic force microscopy, Nucl. Acids Res. 26 (6) (1998) 1473–1480.
[35] R. Krautbauer, H. Clausen-Schaumann, H.E. Gaub, Cisplatin changes the mechanics of single DNA molecules, Angew. Chem. Int. Ed. 39 (21) (2000) 3912.
[36] A. Danesh, X.Y. Chen, M.C. Davies, C.J. Roberts, G.H.W. Sanders, S.J.B. Tendler, P.M. Williams, M.J. Wilkins, The discrimination of drug polymorphic forms from single crystals using atomic force microscopy, Pharm. Res. 17 (7) (2000) 887–890.
[37] C. Thompson, M.C. Davies, C.J. Roberts, S.J.B. Tendler, M.J. Wilkinson, The effects of additives on the growth and morphology of paracetamol (acetaminophen) crystals, Int. J. Pharm. 280 (1–2) (2004) 137–150.
[38] W.K. Burton, N. Cabrera, F.C. Frank, The growth of crystals and the equilibrium structure of their surfaces, Philos. Trans. Roy. Soc. Lond. Philos. Trans. A243 (1951) 299–358.
[39] D. Mahlin, J. Berggren, G. Alderborn, S. Engström, Moisture-induced crystallisation of spray-dried amorphous lactose particles studied by atomic force microscopy, J. Pharm. Sci. 93 (2004) 29–37.
[40] R. Price, P.M. Young, Visualization of the crystallisation of lactose from the amorphous state, J. Pharm. Sci. 93 (2004) 155–164.
[41] J. Wong, A. Chilkoti, V.T. Moy, Direct force measurements of the streptavidin–biotin interaction, Biomol. Eng. 16 (1–4) (1999) 45–55.
[42] M. Radmacher, J.P. Cleveland, M. Fritz, H.G. Hansma, P.K. Hansma, Mapping interaction forces with the atomic force microscope, Biophys. J. 66 (6) (1994) 2159–2165.
[43] A.P. Quist, A.A. Bergman, C.T. Reimann, S.O. Oscarsson, B.U. Sundqvist, Imaging of single antigens, antibodies, and specific immunocomplex formation by scanning force microscopy, Scan. Microsc. 9 (2) (1995) 395–400.
[44] E.L. Florin, V.T. Moy, H.E. Gaub, Adhesion forces between individual ligand–receptor pairs, Science 264 (5157) (1994) 415–417.
[45] A. Chen, V.T. Moy, Cross-linking of cell surface receptors enhances cooperativity of molecular adhesion, Biophys. J. 78 (6) (2000) 2814–2820.
[46] D.W. Pohl, U.C. Fischer, U.T. Durig, Scanning near-field optical microscopy (SNOM), J. Microsc. 152 (1988) 853–861.
[47] D.M. Price, M. Reading, A. Hammiche, H.M. Pollock, Micro-thermal analysis: scanning thermal microscopy and localised thermal analysis, Int. J. Pharm. 192 (1) (1999) 85–96.
[48] K. Six, J. Murphy, I. Weuts, D.Q.M. Craig, G. Verreck, J. Peeters, M. Brewster, G. Van den Mooter, Identification of phase separation in solid dispersions of Itraconazole and Eudragit® E100 using microthermal analysis, Pharm. Res. 20 (1) (2003) 135–138.
[49] E. Meyer, H. Heinzelmann, in: Scanning Tunneling Microscopy II, Springer Ser. Surf. Sci., vol. 28, Springer, Berlin, Heidelberg, 1992, pp. 99–146.
[50] R. Jones, H. Pollock, D. Geldart, A. Verlinden-Luts, Frictional forces between cohesive powder particles studied by AFM, Ultramicroscopy 100 (2004) 59–78.
[51] M. Rasa, B. Kuipers, A. Philipse, Atomic force microscopy and magnetic force microscopy study of model colloids, J. Colloid Interf. Sci. 250 (2002) 303–315.
[52] G. Ge, D. Han, D. Lin, W. Chu, Y. Sun, L. Jiang, W. Ma, C. Wang, MAC mode atomic force microscopy studies of living samples, ranging from cells to fresh tissue, Ultramicroscopy 107 (4–5) (2007) 299–307.
[53] T. Mélin, H. Diesinger, D. Deresmes, D. Stiévenard, Probing nanoscale dipole–dipole interactions by electric force microscopy, Phys. Rev. Lett. 92 (2004) 166101.
[54] H.J. Butt, B. Cappella, M. Kappl, Force measurements with the atomic force microscope: technique, interpretation and applications, Surf. Sci. Rep. 59 (2005) 1–152.
[55] F. Giessibl, S. Hembacher, H. Bielefeldt, J. Mannhart, Subatomic features on the silicon $(1\,1\,1)-(7\times7)$ surface observed by atomic force microscopy, Science 289 (2000) 422–425.
[56] V. Shahin, N.P. Barrera, Providing unique insight into cell biology via atomic force microscopy, Int. Rev. Cytol. 265 (2008) 227–252.
[57] X. Liang, G. Mao, K.Y.S. Ng, Effect of chain lengths of PEO-PPO-PEO on small unilamellar vesicles morphology and stability: an AFM investigation, J. Colloid Interf. Sci. 285 (2005) 360–372.
[58] A. Tarasova, H.J. Griesser, L. Meagher, AFM study of the stability of a dense affinity-bound liposome layer, Langmuir ACS J. Surf. Colloids Sci. 24 (14) (2008) 7371–7377.
[59] H. Bakowsky, T. Richter, C. Kneuer, D. Hoekstra, U. Rothe, G. Bendas, C. Ehrhardt, U. Bakowsky, Adhesion characteristics and stability assessment of lectin-modified liposomes for site-specific drug delivery, Biochim. Biophys. Acta. 1778 (1) (2008) 242–249.
[60] S. Anabousi, E. Kleemann, U. Bakowsky, T. Kissel, T. Schmehl, T. Gessler, W. Seeger, C.M. Lehr, C. Ehrhardt, Effect of PEGylation on the stability of liposomes during nebulisation and in lung surfactant, J. Nanosci. Nanotechnol. 6 (9–10) (2006) 3010–3016.
[61] E. Kleemann, T. Schmehl, T. Gessler, U. Bakowsky, T. Kissel, W. Seeger, Iloprost-containing liposomes for aerosol application in pulmonary arterial hypertension: formulation aspects and stability, Pharm. Res. 24 (2) (2007) 277–287.
[62] I. Schmitz, M. Schreiner, G. Friedbacher, M. Grasserbauer, Phase imaging as an extension to tapping mode AFM for the identification of material properties on humidity-sensitive surfaces, Appl. Surf. Sci. 115 (2) (1997).
[63] R.G. Winkler, J.P. Spatz, S. Sheiko, M. Moller, P. Reineker, O. Marti, Imaging material properties by resonant tapping-force microscopy: a model investigation, Phys. Rev. B. Condens. Matter. 54 (12) (1996) 8908–8912.
[64] W.C. Lin, C.D. Blanchette, T.V. Ratto, M.L. Longo, Lipid asymmetry in DLPC/DSPC-supported lipid bilayers: a combined AFM and fluorescence microscopy study, Biophys. J. 90 (1) (2006) 228–237.
[65] B. Weiss, U.F. Schaefer, J. Zapp, A. Lamprecht, A. Stallmach, C.M. Lehr, Nanoparticles made of fluorescence-labelled poly(L-lactide-co-glycolide): preparation, stability, and biocompatibility, J. Nanosci. Nanotechnol. 6 (2006) 3048–3056.
[66] P. Hinterdorfer, W. Baumgartner, H.J. Gruber, K. Schilcher, H. Schindler, Detection and localization of individual antibody–antigen recognition events by atomic force microscopy, Proc. Natl. Acad. Sci. USA 93 (1996) 3477–3481.
[67] S.A. Gould, K. Burke, P.K. Hansma, Simple theory for the atomic-force microscope with a comparison of theoretical and experimental images of graphite, Phys. Rev. B. Condens. Matter. 40 (8) (1989) 5363–5366.
[68] H.G. Hansma, A.L. Weisenhorn, A.B. Edmundson, H.E. Gaub, P.K. Hansma, Atomic force microscopy: seeing molecules of lipid and immunoglobulin, Clin. Chem. 37 (9) (1991) 1497–1501.
[69] T. Thundat, D.P. Allison, R.J. Warmack, T.L. Ferrell, Imaging isolated strands of DNA molecules by atomic force microscopy, Ultramicroscopy 42–44 (1992) 1101–1106.
[70] T. Thundat, R.J. Warmack, D.P. Allison, L.A. Bottomley, A.J. Lourenco, T.L. Ferrell, Atomic force microscopy of deoxyribonucleic acid strands adsorbed

on mica: the effect of humidity on apparent width and image contrast, J. Vac. Sci. Technol. A10 (1992) 630–635.
[71] T. Thundat, D.P. Allison, R.J. Warmack, G.M. Brown, K.B. Jacobson, J.J. Schrick, T.L. Ferrell, Atomic force microscopy of DNA on mica and chemically modified mica, Scan. Microsc. 6 (4) (1992) 911–918.
[72] S.S. Wong, E. Joselevich, A.T. Woolley, C.L. Cheung, C.M. Lieber, Covalently functionalized nanotubes as nanometre-sized probes in chemistry and biology, Nature 394 (6688) (1998) 52–55.
[73] H.G. Hansma, J. Vesenka, C. Siegerist, G. Keldermann, H. Morrett, R.L. Sinsheimer, V. Elings, C. Bustamante, P.K. Hansma, Reproducible imaging and dissection of plasmid DNA under liquid with the atomic force microscopy, Science 256 (1992) 1180–1184.
[74] H.G. Hansma, R.L. Sinsheimer, M.Q. Li, P.K. Hansma, Atomic force microscopy of single- and double-stranded DNA, Nucl. Acids Res. 20 (14) (1992) 3585–3590.
[75] H.G. Hansma, M. Bezanilla, F. Zenhausern, M. Adrian, R.L. Sinsheimer, Atomic force microscopy of DNA in aqueous solutions, Nucl. Acids Res. 21 (3) (1993) 505–512.
[76] W.M. Heckl, D.P.E. Smith, G. Binnig, H. Klagges, T.W. Hansch, J. Maddocks, Two dimensional ordering of the DNA base Guanine observed with scanning tunneling microscopy, Proc. Nat. Acad. Sci. USA 88 (1991) 8003–8005.
[77] P.A. Ohlsson, T. Tjärnhage, E. Herbai, S. Löfas, G. Puu, Liposome and proteoliposome fusion onto solid substrates, studied using atomic force microscopy, quartz crystal microbalance and surface plasmon resonance. Biological activities of incorporated components, Bioelectrochem. Bioenergy 38 (1995) 137–148.
[78] R.W. Tillmann, U.G. Hofmann, H.E. Gaub, AFM-investigation of the molecular structure of films from a polymerizable two-chain lipid, Chem. Phys. Lipids 73 (1994) 81–89.
[79] D.J. Müller, F.A. Schabert, G. Büldt, A. Engel, Imaging purple membrane in aqueous solutions at sub-nanometer resolution by atomic force microscopy, Biophys. J. 68 (1995) 1681–1686.
[80] O. Marti, V. Elings, M. Haugan, C.E. Bracker, J. Schneir, B. Drake, S.A. Gould, J. Gurley, L. Hellemans, K. Shaw, Scanning probe microscopy of biological samples and other surfaces, J. Microsc. 152 (1988) 803–809.
[81] I.S. Zuhorn, U. Bakowsky, E. Polushkin, W.H. Visser, M.C.A. Stuart, J.B.F.N. Engberts, D. Hoekstra, Nonbilayer phase of lipoplex – membrane mixture determines endosomal escape of genetic cargo and transfection efficiency, Mol. Ther. 11 (5) (2005) 801–810.
[82] V. Oberle, U. Bakowsky, I. Zuhorn, D. Hoekstra, Lipoplex formation under equilibrium conditions reveals a three step mechanism, Biophys. J. 79 (2000) 1447–1454.
[83] V.J. Morris, Biological applications of scanning probe microscopies, Prog. Biophys. Mol. Biol. 61 (1994) 131–185.
[84] D.J. Muller, M. Amrein, A. Engel, Adsorption of biological molecules to a solid support for scanning probe microscopy, J. Struct. Biol. 119 (2) (1997) 172–188.
[85] J.S. Villarrubia, Morphological estimation of tip geometry for scanned probe microscopy, Surf. Sci. 321 (3) (1994) 287–300.
[86] D. Keller, C.H. Chung, Imaging steep, high structures by scanning force microscopy with electron beam deposited tips, Surf. Sci. 268 (1992) 333–339.
[87] M . Micic, A. Chen, R.M. Leblanc, V.T. Moy, Scanning electron microscopy studies of protein-functionalized atomic force microscopy cantilever tips, Scanning 21 (6) (1999) 394–397.
[88] Y. Gu, H. Xie, J. Gao, D. Liu, C.T. Williams, C.J. Murphy, H.J. Ploehn, AFM characterization of dendrimer-stabilized platinum nanoparticles, Langmuir 21 (7) (2005) 3122–3131.
[89] M. Oliva, I. Diez-Perez, P. Gorostiza, C. Lastra, I. Oliva, C. Caramella, E. Marino, Self-assembly of drug-polymer complexes: a spontaneous nanoencapsulation process monitored by atomic force microscopy, J. Pharm. Sci. 92 (1) (2002) 77–83.
[90] A.O. Moughton, R.K. O'Reilly, Noncovalently connected micelles, nanoparticles, and metal-functionalized nanocages using supramolecular self-assembly, J. Am. Chem. Soc. 130 (2008) 8714–8725.
[91] M.R. Almofti, H. Harashima, Y. Shinohara, A. Almofti, Y. Baba, H. Kiwada, Cationic liposome-mediated gene delivery: biophysical study and mechanism of internalization, Arch. Biochem. Biophys. 410 (2) (2003) 246–253.
[92] S. Mao, M. Neu, O. Germershaus, O. Merkel, J. Sitterberg, U. Bakowsky, T. Kissel, Influence of polyethylene glycol chain length on the physicochemical and biological properties of poly(ethylene imine)-graft-poly(ethylene glycol) block copolymer/SiRNA polyplexes, Bioconj. Chem. 17 (5) (2006) 1209–1218.
[93] P. Prabu, A.A. Chaudhari, A. Aryal, N. Dharmaraj, S.Y. Park, W.D. Kim, H.Y. Kim, *In vitro* evaluation of poly(caporlactone) grafted dextran (PGD) nanoparticles with cancer cell, J. Mater. Sci. Mater. Med. 19 (5) (2008) 2157–2163.
[94] Z. Leonenko, E. Finot, M. Amrein, Adhesive interaction measured between AFM probe and lung epithelial type II cells, Ultramicroscope 107 (10–11) (2007) 948–953.
[95] B.Y. Shekunov, P. Chattopadhyay, H.H.Y. Tong, A.H.L. Chow, Particle size analysis in pharmaceutics: principles, methods and applications, Pharm. Res. 24 (2007) 203–227.
[96] K. Oikawa, H. Kim, N. Watanabe, M. Shigeno, Y. Shirakawabe, K. Yasuda, Measuring the sizes of nanospheres on a rough surface by using atomic force microscopy and a curvature-reconstruction method, in: Sensor. Nanostruct., Ultramicroscopy Proceedings of the 8th Int. Conference on Scanning Probe Microscopy 107 (10–11) (2007) 1061–1067.
[97] G. Roe, L. McDonnell, A. Ghanem, A method for measuring the size distribution of latex particles by scanning force microscopy, Ultramicroscope 100 (3–4) (2004) 319–329.
[98] B.M. Lacava, R.B. Azevedo, L.P. Silva, Z.G.M. Lacava, K.S. Neto, N. Buske, A.F. Bakuzis, P.C. Morais, Particle sizing of magnetite-based magnetic fluid using atomic force microscopy: a comparative study with electron microscopy and birefringence, Appl. Phys. Lett. 77 (2000).
[99] D.N. de Assis, V.C.F. Mosqueira, J.M.C. Vilela, M.S. Andrade, V.N. Cardoso, Release profiles and morphological characterization by atomic force microscopy and photon correlation spectroscopy of $^{99m}$Technetium-fluconazole nanocapsules, Int. J. Pharm. 349 (2008) 152–160.
[100] K.L. Wooley, Shell crosslinked polymer assemblies: nanoscale constructs inspired from biological systems, J. Polym. Sci. Part A. Polym. Chem. 38 (9) (2000) 1397–1407.
[101] K. Qi, Q. Ma, E. Remsen, C. Clark Jr., K. Wooley, Determination of the bioavailability of biotin conjugated onto shell crosslinked (SCK) nanoparticles, J. Am. Chem. Soc. 126 (21) (2004) 6599–6607.
[102] Q. Zhang, E. Remsen, K. Wooley, Shell cross-linked nanoparticles containing hydrolytically degradable, crystalline core domains, J. Am. Chem. S. 122 (15) (2000) 3642–3651.
[103] P. Paik, K. Kar, D. Deva, A. Sharma, Measurement of mechanical properties of polymer nanospheres by atomic force microscopy: effects of particle size, Micro Nano Lett. IET 2 (3) (2007) 72–77.
[104] W.H.R.R.S. Stock, J. Polym. Sci.: Polym. Phys. Ed. 23 (1985) 1393.
[105] I. Montasser, H. Fessi, A.W. Coleman, Atomic force microscopy imaging of novel type of polymeric colloidal nanostructures, Eur. J. Pharm. Biopharm. 54 (3) (2002) 281–284.
[106] J. Chatterjee, Y. Haik, C. Chen, Polyethylene magnetic nanoparticle: a new magnetic material for biomedical applications, J. Mag. Mag. Mat. 246 (3) (2002) 382–391.
[107] C. Packhaeuser, T. Kissel, On the design of in situ forming biodegradable parenteral depot systems based on insulin loaded dialkylaminoalkyl-amine-poly(vinyl alcohol)-g-poly(lactide-co-glycolide) nanoparticles, J. Control. Release 123 (2007) 131–140.
[108] O. Germershaus, S. Mao, J. Sitterberg, U. Bakowsky, T. Kissel, Gene delivery using chitosan, trimethyl chitosan or polyethylenglycol-graft-trimethyl chitosan block copolymers: establishment of structure–activity relationships *in vitro*, J. Control. Release 125 (2008) 145–154.
[109] L.A. Dailey, E. Kleemann, M. Wittmar, T. Gessler, T. Schmehl, C. Roberts, W. Seeger, T. Kissel, Surfactant-free, biodegradable nanoparticles for aerosol therapy based on the branched polyesters, DEAPA-PVAL-g-PLGA, Pharm. Res. 20 (12) (2003) 2011–2020.
[110] C. Kneuer, C. Ehrhardt, H. Bakowsky, M.N. Kumar, V. Oberle, C.M. Lehr, D. Hoekstra, U. Bakowsky, The influence of physicochemical parameters on the efficacy of non-viral DNA transfection complexes: a comparative study, J. Nanosci. Nanotechnol. 6 (2006) 2776–2782.
[111] M.N.V.R. Kumar, U. Bakowsky, C.M. Lehr, Preparation and characterization of cationic PLGA nanospheres as DNA carriers, Biomaterials 25 (2004) 1771–1777.
[112] T. Görner, R. Gref, D. Michenot, F. Sommer, M.N. Tran, E. Dellacherie, Lidocaine-loaded biodegradable nanospheres. I. Optimization of the drug incorporation into the polymer matrix, J. Control. Release 57 (3) (1999) 259–268.
[113] B. Yuan, D.A. Wicks, Thermotropic color changing nanoparticles prepared by encapsulating blue polystyrene particles with a poly-N-isopropylacrylamide gel, J. Appl. Poly. Sci. 105 (2007) 446–452.
[114] S. Ramesh, Y. Cohen, D. Aurbach, A. Gedanken, Atomic force microscopy investigation of the surface topography and adhesion of nickel nanoparticles to submicrospherical silica, Chem. Phys. Lett. 287 (1998) 461–467.
[115] L. Mu, S. Feng, A novel controlled release formulation for the anticancer drug paclitaxel (Taxol®): PLGA nanoparticles containing vitamin E TPGS, J. Control. Release 86 (2003) 33–48.
[116] S.S. Feng, L. Mu, K.Y. Win, G. Huang, Nanoparticles of biodegradable polymers for clinical administration of paclitaxel, Curr. Med. Chem. 11 (4) (2004) 413–424.
[117] C. Wang, Y. Zhang, H.S. Seng, L.L. Ngo, Nanoparticle-assisted micropatterning of active proteins on solid substrate, Biosens. Bioelect. 21 (2006) 1638–1643.
[118] W.R. Bowen, P.M. Williams, Dynamic ultrafiltration model for proteins: a colloidal interaction approach, Biotech. Bioeng. 50 (1996) 125–135.
[119] C. Cai, U. Bakowsky, E. Rytting, A.K. Schaper, T. Kissel, Charged nanoparticles as protein delivery systems: a feasibility study using lysozyme as model protein, Eur. J. Pharm. Biopharm. 69 (1) (2008) 31–42.
[120] J. Schäfer, J. Sitterberg, C. Ehrhardt, M.N.V. Ravi Kumar, U. Bakowsky, A new drug vehicle – lipid coated biodegradable nanoparticles, Adv. Sci. Technol. 57 (2008) 148–153.
[121] C.M. Yip, L.M. Brader, B.H. Frank, M.R. DeFelippis, M.D. Ward, Structural studies of a crystalline insulin analog complex with protamine by atomic force microscopy, Biophys. J. 78 (2000) 466–473.
[122] C. Mamot, D.C. Drummond, K. Hong, D.B. Kirpotin, J.W. Park, Liposome-based approaches to overcome anticancer drug resistance, Drug Resist. Updates 6 (2003) 271–279.
[123] S. Ramachandran, A.P. Quist, S. Kumar, R. Lal, Cisplatin nanoliposomes for cancer therapy: AFM and fluorescence imaging of cisplatin encapsulation, stability, cellular uptake, and toxicity, Langmuir 22 (19) (2006) 8156–8162.

[124] J.J. Bergers, T.L.M. Ten Hagen, E.W.M. Van Etten, I.A.J.M. Bakker-Woudenberg, Liposomes as delivery systems in the prevention and treatment of infectious diseases, Pharm. World Sci. 17 (2005) 1–11.
[125] M.R. Niesman, The use of liposomes as drug carriers in ophthalmology, Crit. Rev. Ther. Drug Carr. Syst. 9 (1) (1992) 1–38.
[126] M. Gaspar, U. Bakowsky, C. Ehrhardt, Inhaled liposomes – current strategies and future challenges, J. Biomed. Nanotechnol. 4 (3) (2008) 245–257.
[127] M.M. Gaspar, O.C. Boerman, P. Laverman, M.L. Corvo, G. Storm, M.E. Cruz, Enzymosomes with surface-exposed superoxide dismutase: *in vivo* behaviour and therapeutic activity in a model of adjuvant arthritis, J. Control. Release 117 (2) (2007) 186–195.
[128] S. Anabousi, U. Bakowsky, M. Schneider, H. Huwer, C.M. Lehr, C. Ehrhardt, *In vitro* assessment of transferrin-conjugated liposomes as drug delivery systems for inhalation therapy of lung cancer, Eur. J. Pharm. Sci. 29 (5) (2006) 367–374.
[129] G. Sharma, S. Anabousi, C. Ehrhardt, M.N. Ravi Kumar, Liposomes as targeted drug delivery systems in the treatment of breast cancer, J. Drug. Target. 14 (5) (2006) 301–310.
[130] S. Anabousi, M. Laue, C.M. Lehr, U. Bakowsky, C. Ehrhardt, Assessing transferrin modification of liposomes by atomic force microscopy and transmission electron microscopy, Eur. J. Pharm. Biopharm. 60 (2) (2005) 295–303.
[131] V.P. Torchilin, Recent advances with liposomes as pharmaceutical carriers, Nat. Rev. Drug Discov. 4 (2005) 145–159.
[132] P. Vermette, L. Meagher, E. Gagnon, H.J. Griesser, C.J. Doillon, Immobilized liposome layers for drug delivery applications: inhibition of angiogenesis, J. Control. Release 80 (1–3) (2002) 179–195.
[133] V.A. Carmo, M.C. De Oliveira, E.C. Reis, T.M. Guimarães, J.M. Vilela, M.S. Andrade, M.S. Michalick, V.N. Cardoso, Physicochemical characterization and study of *in vitro* interactions of pH-sensitive liposomes with the complement system, J. Liposome Res. 18 (1) (2008) 59–70.
[134] G. Bendas, A. Krause, U. Bakowsky, J. Vogel, U. Rothe, Targetability of novel immunoliposomes prepared by a new antibody conjugation technique, Int. J. Pharm. 181 (1) (1999) 79–93.
[135] K. Nakano, Y. Tozuka, H. Yamamoto, Y. Kawashima, H.A. Takeuchi, A novel method for measuring rigidity of submicron-size liposomes with atomic force microscopy, Int. J. Pharm. 355 (1–2) (2008) 203–209.
[136] K. Sakai, H. Tomizawa, K. Tsuchiya, N. Ishida, H. Sakai, M. Abe, Characterizing the structural transition of cationic DPPC liposomes from the approach of TEM, SAXS and AFM measurements, Colloids. Surf. B. Biointerf. 67 (1) (2008) 73–78.
[137] X. Liang, G. Mao, K.Y. Ng, Mechanical properties and stability measurement of cholesterol containing liposomes on mica by atomic force microscopy, J. Colloid. Interf. Sci. 278 (1) (2004) 53–62.
[138] B. Ruozi, G. Tosi, F. Forni, M. Fresta, M.A. Vandelli, Atomic force microscopy and photon correlation spectroscopy: two techniques for rapid characterization of liposomes, Eur. J. Pharm. Sci. 25 (1) (2005) 81–89.
[139] A. Berquand, N. Fa, Y.F. Dufrêne, M.P. Mingeot-Leclercq, Interaction of the macrolide antibiotic azithromycin with lipid bilayers: effect on membrane organization, fluidity, and permeability, Pharm. Res. 22 (3) (2005) 465–475.
[140] N. Fa, L. Lins, P.J. Courtoy, Y. Dufrêne, P. Van Der Smissen, R. Brasseur, D. Tyteca, M.P. Mingeot-Leclercq, Decrease of elastic moduli of DOPC bilayers induced by a macrolide antibiotic, azithromycin, Biochim. Biophys. Acta. 1768 (7) (2007) 1830–1838.
[141] I.S. Zuhorn, V. Oberle, W.H. Visser, J.B. Engberts, U. Bakowsky, E. Polushkin, D. Hoekstra, Phase behavior of cationic amphiphiles and their mixtures with helper lipid influences lipoplex shape, DNA translocation, and transfection efficiency, Biophys. J. 83 (4) (2002) 2096–2108.
[142] R. Marty, C.N. N'soukpoé-Kossi, D. Charbonneau, C.M. Weinert, L. Kreplak, H.A. Tajmir-Riahi, Structural analysis of DNA complexation with cationic lipids, Nucl. Acids Res. (2008) (Epub ahead of print).
[143] C. Kawaura, A. Noguchi, T. Furuno, M. Nakanishi, Atomic force microscopy for studying gene transfection mediated by cationic liposomes with a cationic cholesterol derivative, FEBS Lett. 421 (1) (1998) 69–72.
[144] Y.Z. Zhao, Y.K. Luo, H.D. Liang, X.G. Mei, J. Tang, C.T. Lu, Y. Zhang, Q. Lin, Comparing transfection efficiency and safety for antisense oligodeoxyribonucleotide between phospholipids-based microbubbles and liposomes, J. Drug Target. 4 (10) (2006) 687–693.
[145] M.A. Wolfert, L.W. Seymour, Atomic force microscopic analysis of the influence of the molecular weight of poly(L)lysine on the size of polyelectrolyte complexes formed with DNA, Gene Ther. 3 (1996) 269–273.
[146] M.A. Wolfert, E.H. Schacht, V. Toncheva, K. Ulbrich, O. Nazarova, L.M. Seymour, Characterization of vectors for gene therapy formed by self-assembly of DNA with synthetic block co-polymers, Hum. Gene Ther. 7 (1996) 2123–2133.
[147] S. Werth, B. Urban-Klein, L. Dai, S. Hobel, M. Grzelinski, U. Bakowsky, F. Czubayko, A. Aigner, A low molecular weight fraction of polyethylenimine (PEI) displays increased transfection efficiency of DNA and siRNA in fresh or lyophilized complexes, J Control. Release 112 (2) (2006) 257–270.
[148] C.G. Oster, M. Wittmar, U. Bakowsky, T. Kissel, DNA nano-carriers from biodegradable cationic branched polyesters are formed by a modified solvent displacement method, J. Control. Release 111 (3) (2006) 371–381.
[149] T. Merdan, K. Kunath, H. Petersen, U. Bakowsky, K.H. Voigt, J. Kopecek, T. Kissel, PEGylation of poly(ethylene imine) affects stability of complexes with plasmid DNA under *in vivo* conditions in a dose-dependent manner after intravenous injection into mice, Bioconjug. Chem. 16 (4) (2005) 785–792.
[150] T. Merdan, J. Callahan, H. Petersen, K. Kunath, U. Bakowsky, P. Kopeckova, T. Kissel, J. Kopecek, Pegylated polyethylenimine-Fab' antibody fragment conjugates for targeted gene delivery to human ovarian carcinoma cells, Bioconj. Chem. 14 (5) (2003) 989–996.
[151] Y.T. Chim, J.K. Lam, Y. Ma, S.P. Armes, A.L. Lewis, C.J. Roberts, S. Stolnik, S.J. Tendler, M.C. Davies, Structural study of DNA condensation induced by novel phosphorylcholine-based copolymers for gene delivery and relevance to DNA protection, Langmuir 21 (8) (2005) 3591–3598.
[152] M. Neu, J. Sitterberg, U. Bakowsky, T. Kissel, Stabilized nanocarriers for plasmids based upon cross-linked poly(ethylene imine), Biomacromolecules 7 (12) (2006) 3428–3438.
[153] U. Bakowsky, J. Sitterberg, Understanding nanoscale drug delivery systems, Glatt Int. Times. 23 (2007) 19–23.
[154] A.L. Martin, M.C. Davies, B.J. Rackstraw, C.J. Roberts, S. Stolnik, S.J.B. Tendler, P.M. Williams, Observation of DNA-polymer condensate formation in real time at a molecular level, FEBS Lett. 480 (2000) 106–112.
[155] H.G. Abdelhady, S. Allen, M.C. Davies, C.J. Roberts, S.J.B. Tendler, P.M. Williams, Direct real-time molecular scale visualisation of the degradation of condensed DNA complexes exposed to DNase I, Nucl. Acids Res. 31 (14) (2003) 4001–4005.
[156] M. Grzelinski, B. Urban-Klein, T. Martens, K. Lamszus, U. Bakowsky, S. Höbel, F. Czubayko, A. Aigner, RNA interference-mediated gene silencing of pleiotrophin through polyethylenimine-complexed small interfering RNAs *in vivo* exerts antitumoral effects in glioblastoma xenografts, Human Gene Ther. 17 (7) (2006) 751–766.
[157] S.S. Pennadam, J.S. Ellis, M.D. Lavigne, D.C. Górecki, M.C. Davies, C. Alexander, Synthesis and characterization of variable-architecture thermosensitive polymers for complexation with DNA, Langmuir 23 (1) (2007) 41–49.
[158] E. Kleemann, L.A. Dailey, H.G. Abdelhady, T. Gessler, T. Schmehl, C.J. Roberts, M.C. Davies, W. Seeger, T. Kissel, Modified polyethylenimines as non-viral gene delivery systems for aerosol gene therapy: investigations of the complex structure and stability during air-jet and ultrasonic nebulization, J. Control. Release 100 (3) (2004) 437–450.
[159] C. Peetla, V. Labhasetwar, Biophysical characterization of nanoparticle–endothelial model cell membrane interactions, Mol. Pharm. 5 (3) (2008) 418–429.
[160] P.R. Leroueil, S.A. Berry, K. Duthie, G. Han, V.M. Rotello, D.Q. McNerny, J.R. Baker Jr., B.G. Orr, M.M. Holl, Wide varieties of cationic nanoparticles induce defects in supported lipid bilayers, Nano Lett. 8 (2008) 420–424.
[161] S. Kanno, A. Furuyama, S. Hirano, A murine scavenger receptor MARCO recognizes polystyrene nanoparticles, Toxicol. Sci. 97 (2) (2007) 398–406.
[162] Y.L. Pan, J.Y. Cai, L. Qin, H. Wang, Atomic force microscopy-based cell nanostructure for ligand-conjugated quantum dot endocytosis, Acta. Biochim. Biophys. Sin (Shanghai) 38 (9) (2006) 646–652.